NATIONAL ADVISORY COMMITTEE FOR AERONAUTICS

TECHNICAL NOTE 3347

A WIND-TUNNEL TEST TECHNIQUE FOR MEASURING THE DYNAMIC ROTARY STABILITY DERIVATIVES INCLUDING THE CROSS DERIVATIVES AT HIGH MACH NUMBERS

By Benjamin H. Beam

Ames Aeronautical Laboratory
Moffett Field, Calif.

Washington
January 1955

NATIONAL ADVISORY COMMITTEE FOR AERONAUTICS

TECHNICAL NOTE 3347

A WIND-TUNNEL TEST TECHNIQUE FOR MEASURING THE DYNAMIC ROTARY STABILITY DERIVATIVES INCLUDING THE CROSS DERIVATIVES AT HIGH MACH NUMBERS

By Benjamin H. Beam

SUMMARY

A method is described for measuring the dynamic stability derivatives of a model airplane in a wind tunnel. The characteristic features of this system are that single-degree-of-freedom oscillations were used to obtain combinations of rolling, yawing, and pitching motions; that the oscillations were excited and controlled by velocity feedback which permitted operation under conditions unfavorable for more conventional types of oscillatory testing; and that data processing was greatly simplified by using analog computer elements in the strain-gage circuitry.

The system described is primarily for measurement of the damping derivatives C_{l_p} (damping in roll), $C_{m_q} + C_{m_{\dot{\alpha}}}$ (damping in pitch), $C_{n_r} - C_{n_{\dot{\beta}}}$ (damping in yaw), and the cross derivatives $C_{l_r} - C_{l_{\dot{\beta}}}$ (rolling moment due to yawing) and C_{n_p} (yawing moment due to rolling). The method of testing also permits measurement under oscillatory conditions of the static derivatives C_{l_β} (rolling moment due to sideslip), C_{n_β} (yawing moment due to sideslip), and C_{m_α} (pitching moment due to angle of attack). All these derivatives are of particular importance in estimating the short-period oscillatory motions of a rigid airplane.

A small number of experimental data are included to illustrate the general scope of results obtainable with this system.

INTRODUCTION

One important problem in the dynamic motions of airplanes is the nature and the stability of the oscillatory modes. In measuring the dynamic stability derivatives which apply to these motions there are certain advantages in employing oscillation methods in a wind tunnel, and the development of such methods has always been attractive to investigators. Most of the early measurements of damping in pitch were made from oscillation tests of a model in a wind tunnel. Damping in roll and

damping in yaw have also been measured in this way but, in general, experimental difficulties have prevented the wide application of this method to the lateral motions. This is particularly true in the case of the cross derivatives, yawing moment due to rolling, and rolling moment due to yawing, although in one recently developed method (ref. 1) the yawing moment due to rolling has been successfully measured using a two-degree-of-freedom oscillatory technique.

Most of the studies of the lateral derivatives have been made on the basis of steady turning or rolling motions. Theoretical calculations of the derivatives are largely based on this assumption. The steady turning or rolling flow technique has been used in the systematic studies of the lateral derivatives in the Langley stability tunnel (e.g., refs. 2 and 3). Curved or rolling flight is approximated in the test section of this wind tunnel by causing the air to follow a curved or spiral path past a fixed model. At high speeds, the rolling derivatives have been measured by steadily rotating a sting-mounted model in a wind tunnel with a dynamometer and measuring the damping in roll, yawing moment due to rolling, and the side force due to rolling. These methods and other techniques have been described and referred to in various NACA publications on the stability derivatives for airplane and missile configurations.

The purpose of this report is to describe an oscillation technique for measuring the lateral and longitudinal dynamic stability derivatives in a wind tunnel. It was developed primarily for testing at high subsonic or supersonic speeds and for this reason three features are believed to be of special interest. One of these is the single-degree-of-freedom oscillatory system in which various components of pitch, roll, and yaw were obtained by varying the axis of oscillation. Second, the forcing system comprised a feedback loop in which velocity feedback was used to excite and control the amplitude of the model oscillation. A third feature is a system of strain-gage data processing in which electronic analog computer elements were used in measuring the amplitude and phase position of the oscillatory strain-gage deflections. The advice and assistance of the instrument development branch was extremely valuable in developing this system of data processing.

The test apparatus is capable of measuring the moment derivatives which arise from angular motions of the airplane. This includes the rotary damping derivatives C_{l_p}, $C_{m_q} + C_{m_{\dot{\alpha}}}$, and $C_{n_r} - C_{n_{\dot{\beta}}}$; the cross derivatives C_{n_p} and $C_{l_r} - C_{l_{\dot{\beta}}}$; and the displacement derivatives C_{l_β}, C_{n_β}, and C_{m_α}. These derivatives are of particular importance in estimating the short-period oscillatory motions of a rigid airplane.

DEFINITIONS AND SYMBOLS

Two systems of axes are used in this analysis. The stability system of axes with the positive directions of moments and angles referred to this system are illustrated in figure 1. The oscillation axes used for wind-tunnel measurements are illustrated in figure 2 and defined with respect to the stability axes by a set of direction cosines. Primes are used with aerodynamic moment and axis designations referred to the oscillation system of axes.

The various stability derivatives are defined as follows:

$$C_{l_p} \quad \frac{2}{\rho V^2 S b} \frac{\partial L}{\partial \frac{pb}{2V}}$$

$$C_{n_p} \quad \frac{2}{\rho V^2 S b} \frac{\partial N}{\partial \frac{pb}{2V}}$$

$$C_{l_r} \quad \frac{2}{\rho V^2 S b} \frac{\partial L}{\partial \frac{rb}{2V}}$$

$$C_{n_r} \quad \frac{2}{\rho V^2 S b} \frac{\partial N}{\partial \frac{rb}{2V}}$$

$$C_{m_q} \quad \frac{2}{\rho V^2 S \bar{c}} \frac{\partial M}{\partial \frac{q\bar{c}}{2V}}$$

$$C_{m_\alpha} \quad \frac{2}{\rho V^2 S \bar{c}} \frac{\partial M}{\partial \alpha}$$

$$C_{m_{\dot{\alpha}}} \quad \frac{2}{\rho V^2 S \bar{c}} \frac{\partial M}{\partial \frac{\dot{\alpha}\bar{c}}{2V}}$$

$$C_{l_\beta} \quad \frac{2}{\rho V^2 S b} \frac{\partial L}{\partial \beta}$$

$$C_{n_\beta} \quad \frac{2}{\rho V^2 S b} \frac{\partial N}{\partial \beta}$$

$$C_{l_{\dot{\beta}}} \quad \frac{2}{\rho V^2 Sb} \frac{\partial L}{\partial \frac{\dot{\beta} b}{2V}}$$

$$C_{n_{\dot{\beta}}} \quad \frac{2}{\rho V^2 Sb} \frac{\partial N}{\partial \frac{\dot{\beta} b}{2V}}$$

$$C_{l'_{\sigma}} \quad \frac{2}{\rho V^2 Sb} \frac{\partial L'}{\partial \sigma}$$

$$C_{m'_{\sigma}} \quad \frac{2}{\rho V^2 Sb} \frac{\partial M'}{\partial \sigma}$$

$$C_{n'_{\sigma}} \quad \frac{2}{\rho V^2 Sb} \frac{\partial N'}{\partial \sigma}$$

$$C_{l'_{\dot{\sigma}}} \quad \frac{2}{\rho V^2 Sb} \frac{\partial L'}{\partial \frac{\dot{\sigma} b}{2V}}$$

$$C_{m'_{\dot{\sigma}}} \quad \frac{2}{\rho V^2 Sb} \frac{\partial M'}{\partial \frac{\dot{\sigma} b}{2V}}$$

$$C_{n'_{\dot{\sigma}}} \quad \frac{2}{\rho V^2 Sb} \frac{\partial N'}{\partial \frac{\dot{\sigma} b}{2V}}$$

The following symbols are used in the report:

A,B,. . ., H,J	direction cosines between primed and unprimed axes
I	moment or product of inertia, depending on subscript, positive where negative moment results from positive acceleration, slug-ft^2
K	mechanical spring constant, positive where negative moment results from positive deflection, ft-lb/radian
L	aerodynamic rolling moment, ft-lb
M	aerodynamic pitching moment, ft-lb

N	aerodynamic yawing moment, ft-lb
P	mechanical damping-moment coefficient, positive where negative moment results from positive velocity, ft-lb sec/radian
R	resistance, ohms
S	wing area, sq ft
T	torque, ft-lb
V	air velocity, ft/sec
b	wing span, ft
$\bar{c}$	mean aerodynamic chord, ft
e	voltage, volts
f	frequency of sinusoidal oscillation, cps
g	transfer function, $\frac{\text{output}}{\text{input}}$
i	galvanometer current, amp
k	strain-gage calibration constant, amp/volt/unit load
p	rolling velocity, radians/sec
q	pitching velocity, radians/sec
r	yawing velocity, radians/sec
t	time, sec
x,y,z	stability system of axes, defined in figure 1
x',y',z'	system of axes used for oscillation tests, defined with respect to the stability axes by the direction cosines
α	angle of attack, radians
α_m	mean or static angle of attack, deg
β	angle of sideslip, radians except where noted
θ	pitch angle, radians
φ	roll angle, radians

ψ	yaw angle, radians
σ	angle of rotation of model about x' axis, radians except where noted
ϵ	small angular displacement about y' or z' axis, radians
η, λ	direction angles, defined in figure 2, deg
μ, ν, ξ	phase angles of σ, $T_{x'}$, and $\epsilon_{y'}$ with respect to an arbitrary reference
ρ	air density, slugs/cu ft
ω	circular frequency of oscillation, $2\pi f$, radians/sec
ω_o	wind-off circular frequency of oscillation, radians/sec
$\dot{(\ )}$	$\frac{d(\ )}{dt}$
$\ddot{(\ )}$	$\frac{d^2(\ )}{dt^2}$
$\bar{(\ )}$	maximum value of a sinusoidally oscillating quantity ( )
$\Delta(\ )$	incremental value of a quantity ( )

Subscripts define the particular axis or motion to which the general symbol applies.

THEORY

Single-Degree-of-Freedom Oscillatory System

The general dynamic motion of a rigid airplane with no moving control surfaces requires six differential equations. Three of these define translation and three define rotation about the center of gravity. If the center of gravity of a model airplane is fixed in a wind tunnel, the equations involving translation can be eliminated and the motion is defined in terms of rotary motions and derivatives by three equations. The system can be further restrained so that rotation occurs about one arbitrary fixed axis only. In this case the motion is defined by one equation even though simultaneous rolling, pitching, and yawing motions may be involved.

Assume an orthogonal coordinate system, the x'y'z' system (fig. 2), the origin of which is at the center of gravity of the model airplane and in which rotation of the model is always about the x' axis. Equilibrium

requires that the summation of the moments about the x', y', and z' axes be equal to zero. The equation for small angular oscillations about a static equilibrium condition can be written in terms of a single variable

$$- I_{x'x'}\ddot{\sigma} - P_{x'}\dot{\sigma} - K_{x'}\sigma + \Delta L' + T_{x'} = 0 \tag{1}$$

The sign convention of figure 2 requires that if $I_{x'x'}$, $P_{x'}$, and $K_{x'}$ are considered positive quantities, their respective moments must be prefixed by a negative sign since they oppose the motion. The quantity $\Delta L'$ is the sum of all aerodynamic moments about the axis of oscillation arising from angular deflection, velocity, acceleration, etc., about the static equilibrium condition. The aerodynamic moments due to angular acceleration and higher-order terms are generally neglected in stability calculations, permitting the assumption that

$$\Delta L' = \frac{\partial L'}{\partial \sigma}\sigma + \frac{\partial L'}{\partial \dot{\sigma}}\dot{\sigma} \tag{2}$$

$$= \frac{1}{2}\rho V^2 Sb\left(\frac{b}{2V} C_{l'_{\dot{\sigma}}}\dot{\sigma} + C_{l'_{\sigma}}\sigma\right) \tag{3}$$

and equation (1) could be written

$$I_{x'x'}\ddot{\sigma} + \left(P_{x'} - \frac{1}{4}\rho VSb^2 C_{l'_{\dot{\sigma}}}\right)\dot{\sigma} + \left(K_{x'} - \frac{1}{2}\rho V^2 Sb\, C_{l'_{\sigma}}\right)\sigma = T_{x'} \tag{4}$$

It is apparent from the left-hand side of equation (4) that $C_{l'_{\dot{\sigma}}}$ is an aerodynamic damping coefficient and that a negative value of $C_{l'_{\dot{\sigma}}}$ would result in a positively damped oscillation. A negative value of the coefficient $C_{l'_{\sigma}}$ would result in a positive restoring moment about the axis of oscillation. This sign convention is thus parallel to that of the stability derivatives about the stability axes.

Equations expressing the equilibrium of moments about the y' and z' axes for small oscillations about the x' axis can also be written

$$- I_{x'y'}\ddot{\sigma} + \Delta M' - K_{y'}\epsilon_{y'} = 0 \tag{5}$$

$$- I_{x'z'}\ddot{\sigma} + \Delta N' - K_{z'}\epsilon_{z'} = 0 \tag{6}$$

Equations (5) and (6) can be written in this simple form only if $\epsilon_{y'}$ and $\epsilon_{z'}$ are sufficiently small compared with σ that their effects are negligible in equations (1), (5), and (6) except for the terms $K_{y'}\epsilon_{y'}$ and $K_{z'}\epsilon_{z'}$. This is accomplished by limiting $\epsilon_{y'}$ and $\epsilon_{z'}$ to very small values but making $K_{y'}$ and $K_{z'}$ very large. In other words, the model would be relatively easy to deflect about the x' axis but very stiff about the y' and z' axes. From a development similar to that of equations (3) and (4) it can be shown that

$$- I_{x'y'}\ddot{\sigma} + \frac{1}{2}\rho V^2 Sb\left(\frac{b}{2V} C_{m'_{\dot{\sigma}}}\dot{\sigma} + C_{m'_{\sigma}}\sigma\right) = K_{y'\epsilon_{y'}} \tag{7}$$

$$- I_{x'z'}\ddot{\sigma} + \frac{1}{2}\rho V^2 Sb\left(\frac{b}{2V} C_{n'_{\dot{\sigma}}}\dot{\sigma} + C_{n'_{\sigma}}\sigma\right) = K_{z'\epsilon_{z'}} \tag{8}$$

The values of the aerodynamic coefficients in equations (4), (7), and (8) will change with the orientation of the oscillation axes in the wind tunnel and the attitude of the model with respect to the air stream. These changes are related to changes in magnitude and relative contribution of the stability derivatives, ordinarily measured about the stability axes defined in figure 1. The geometric relation between the oscillation system of axes (the x'y'z' system) and the stability axes (the xyz system) is completely defined by the direction cosines between the two systems. These can be symbolized in the following matrix form

	x'	y'	z'
x	A	D	G
y	B	E	H
z	C	F	J

(9)

where, for example, the cosine of the angle between the y and z' axes is H.

The numerical evaluation of these direction cosines is somewhat complicated since the stability axes do not remain fixed with respect to the oscillation axes as the angle of attack is changed, as is apparent from a study of figures 1 and 2. It will be shown later in the Appendix that certain simplifications are possible in numerical calculations by a less direct approach through a set of model axes. Since, however, in the present discussion the direction cosines are considered only in symbolic form, it is not necessary to introduce this additional step.

Small angular motions about the axis of oscillation can be resolved into component motions of roll, pitch, and yaw about the stability axes. The relative magnitude of each component depends on the direction cosine between the x' axis and the roll, pitch, or yaw axes, and, with the approximations sin $\sigma = \sigma$, cosine $\sigma = 1$,

$$\left.\begin{aligned} \Delta\varphi &= A\sigma \quad & \dot{\varphi} &= p = A\dot{\sigma} \\ \Delta\theta &= B\sigma \quad & \dot{\theta} &= q = B\dot{\sigma} \\ \Delta\psi &= C\sigma \quad & \dot{\psi} &= r = C\dot{\sigma} \end{aligned}\right\} \tag{10}$$

The moments about the stability axes can be expressed in terms of the aerodynamic stability derivatives

$$\Delta L = \frac{1}{2}\rho V^2 Sb \left[\frac{b}{2V}\left(C_{l_p}\dot{\varphi} + C_{l_r}\dot{\psi} + C_{l_{\dot{\beta}}}\dot{\beta}\right) + C_{l_\beta}(\Delta\beta)\right] \tag{11}$$

$$\Delta M = \frac{1}{2}\rho V^2 S\bar{c} \left[\frac{\bar{c}}{2V}\left(C_{m_q}\dot{\theta} + C_{m_{\dot{\alpha}}}\dot{\alpha}\right) + C_{m_\alpha}(\Delta\alpha)\right] \tag{12}$$

$$\Delta N = \frac{1}{2}\rho V^2 Sb \left[\frac{b}{2V}\left(C_{n_p}\dot{\varphi} + C_{n_r}\dot{\psi} + C_{n_{\dot{\beta}}}\dot{\beta}\right) + C_{n_\beta}(\Delta\beta)\right] \tag{13}$$

For straight flight, as in the wind tunnel, $\alpha = \theta$ and $\beta = -\psi$. The aerodynamic moments can then be referred back to the oscillation system of axes through the direction cosines.

$$\Delta L' = A(\Delta L) + B(\Delta M) + C(\Delta N) \tag{14}$$

$$\Delta M' = D(\Delta L) + E(\Delta M) + F(\Delta N) \tag{15}$$

$$\Delta N' = G(\Delta L) + H(\Delta M) + J(\Delta N) \tag{16}$$

Thus, the aerodynamic moments indicated in equations (1), (5), and (6) for oscillation about an arbitrary axis are defined in terms of moments about the stability axes by equations (14), (15), and (16). The aerodynamic coefficients which depend on the angular velocity of the model can be derived in terms of the stability derivatives as

$$C_{l'_{\dot{\sigma}}} = \frac{2}{\rho V^2 Sb}\frac{\partial L'}{\partial \frac{\dot{\sigma}b}{2V}}$$

$$= A^2 C_{l_p} + AC\left(C_{n_p} + C_{l_r} - C_{l_{\dot{\beta}}}\right) + B^2\frac{\bar{c}^2}{b^2}\left(C_{m_q} + C_{m_{\dot{\alpha}}}\right) + C^2\left(C_{n_r} - C_{n_{\dot{\beta}}}\right) \tag{17}$$

$$C_{m'_{\dot{\sigma}}} = ADC_{l_p} + CD\left(C_{l_r} - C_{l_{\dot{\beta}}}\right) + EB\frac{\bar{c}^2}{b^2}\left(C_{m_q} + C_{m_{\dot{\alpha}}}\right) + AFC_{n_p} + FC\left(C_{n_r} - C_{n_{\dot{\beta}}}\right) \tag{18}$$

$$C_{n'_{\dot{\sigma}}} = AGC_{l_p} + CG\left(C_{l_r} - C_{l_{\dot{\beta}}}\right) + HB\frac{\bar{c}^2}{b^2}\left(C_{m_q} + C_{m_{\dot{\alpha}}}\right) + AJC_{n_p} + CJ\left(C_{n_r} - C_{n_{\dot{\beta}}}\right) \tag{19}$$

Those coefficients which depend on displacement of the model become

$$C_{l'_\sigma} = \frac{2}{\rho V^2 Sb} \frac{\partial L'}{\partial \sigma}$$

$$= - ACC_{l_\beta} + B^2 \frac{\bar{c}}{b} C_{m_\alpha} - C^2 C_{n_\beta} \tag{20}$$

$$C_{m'_\sigma} = - DCC_{l_\beta} + EB \frac{\bar{c}}{b} C_{m_\alpha} - FCC_{n_\beta} \tag{21}$$

$$C_{n'_\sigma} = - GCC_{l_\beta} + HB \frac{\bar{c}}{b} C_{m_\alpha} - JCC_{n_\beta} \tag{22}$$

In equation (17) $C_{l'_{\dot{\sigma}}}$ is the aerodynamic damping coefficient measured about the axis of oscillation in the wind tunnel. If the x' axis coincides with the x axis the oscillation would be pure roll. In this case $A^2 = 1$ and $AC = B^2 = C^2 = 0$ so the measured damping coefficient would be C_{l_p}, the damping-in-roll coefficient. Similarly, a pure pitching or yawing oscillation would result in the measurement of damping in pitch or damping in yaw.

In general, one stability derivative can be obtained from each separate physical measurement. In equations (17), (18), and (19) there are eight stability derivatives which depend on angular velocity; however, these derivatives form only five independent terms. The derivative C_{m_q} always appears with $C_{m_{\dot{\alpha}}}$ in the above since, for the pure rotary motions considered, q is always equal to $\dot{\alpha}$. (See ref. 4.) Similarly, since $r = - \dot{\beta}$ in a test of this type, $C_{l_r} - C_{l_{\dot{\beta}}}$ appears as one term and $C_{n_r} - C_{n_{\dot{\beta}}}$ as another. The evaluation of these five terms (C_{l_p}, C_{n_p}, $C_{m_q} + C_{m_{\dot{\alpha}}}$, $C_{l_r} - C_{l_{\dot{\beta}}}$, and $C_{n_r} - C_{n_{\dot{\beta}}}$) requires five unique measurements.

Equations (17), (18), and (19) can be considered in a purely formal way as the basis for a system of equations containing the unknown stability derivatives. Assuming that five values of $C_{l'_{\dot{\sigma}}}$, $C_{m'_{\dot{\sigma}}}$, or $C_{n'_{\dot{\sigma}}}$ are available from wind-tunnel measurements, along with the appropriate direction cosines for the axes about which the measurements were made, a system of five equations could be formed. These equations could then be solved simultaneously for the five stability derivatives, providing the equations are mathematically determinate.

The necessary values of $C_{l'_{\dot{\sigma}}}$, $C_{m'_{\dot{\sigma}}}$, or $C_{n'_{\dot{\sigma}}}$ which lead to the velocity derivatives and $C_{l'_\sigma}$, $C_{m'_\sigma}$, or $C_{n'_\sigma}$ which lead to the static derivatives are obtained from physical measurements of the model oscillation through equations (4), (7), and (8). Measurements can be made of the frequency of oscillation ω, the input torque $T_{x'}$, the oscillation amplitude σ, and the small angular deflections $\epsilon_{y'}$ and $\epsilon_{z'}$. There is considerable latitude in the choice of axes of oscillation and the particular quantities to be

measured within the general confines of mathematical determinateness of the stability derivatives. Note, however, that $\epsilon_{y'}$ and $\epsilon_{z'}$ are inherently more difficult to measure than σ. The small displacements and high stiffness required about the y' and z' axes to maintain the validity of equations (4), (7), and (8) impose a limitation on the accuracy of measurements about these axes. Friction, backlash, and interaction become of increasing importance as the displacement is reduced. Some measurements must be made in conjunction with large static pitching moments or aerodynamic disturbances of a random nature and these factors will affect the design of the apparatus and the accuracy of the system.

For the oscillation apparatus discussed herein it was decided to avoid measurements of $\epsilon_{y'}$ and $\epsilon_{z'}$ where possible in favor of σ. The arrangement was such that all the stability derivatives discussed except C_{n_p} and C_{l_r} could be determined from measurements of ω, $T_{x'}$, and σ in a series of four tests in which all test conditions remained constant except for changes in the axis of oscillation. From these measurements also, a value could be obtained for the sum $C_{n_p} + C_{l_r} - C_{l_{\dot{\beta}}}$. Therefore, one additional measurement was required to resolve these two derivatives. This was obtained by measuring $\epsilon_{y'}$ during one of the four tests, which provided an accurate resolution of C_{n_p} because in this case the moments due to the other aerodynamic derivatives had little effect on $\epsilon_{y'}$. The direction cosines which identify the axes of oscillation used are given in the Appendix. These can be used to form the simultaneous equations needed to evaluate the stability derivatives. The method used to relate the measurements of $T_{x'}$, ω, σ, and $\epsilon_{y'}$ to the derivatives $C_{l'_{\dot{\sigma}}}$, $C_{n'_{\dot{\sigma}}}$, etc., is discussed in subsequent sections.

Feedback Control

As indicated in the preceding section, measurement of the aerodynamic derivatives depends upon an analysis of a single-degree-of-freedom oscillation defined by equation (4) repeated here for convenience.

$$I_{x'x'}\ddot{\sigma} + \left(P_{x'} - \frac{1}{4}\rho V S b^2 C_{l'_{\dot{\sigma}}}\right)\dot{\sigma} + \left(K_{x'} - \frac{1}{2}\rho V^2 S b\, C_{l'_{\sigma}}\right)\sigma = T_{x'} \quad (4)$$

In the case of a free oscillation $T_{x'}$ would become zero and the oscillation would be a damped sinusoid. Use of this method is generally limited to test conditions which would not result in oscillatory instability as there is no control over the amplitude once the oscillation is initiated.

For the forced oscillation, $T_{x'}$ in equation (4) is a sinusoidal function of time. One case of interest is where the frequency of the applied torque corresponds to the undamped natural frequency of the oscillatory system. At this frequency the inertia moments balance the restoring

moments and the final amplitude after the decay of initial transients corresponds to a balance between the damping moments and the applied torque. The maximum angular velocity of oscillation can be obtained with a minimum of input torque at this frequency, as the entire input is used to overcome the damping. It is thus a desirable operating point both from the standpoint of power requirements and accuracy in measuring the damping.

One disadvantage of the forced-oscillation method is that, as with the free-oscillation system, testing cannot be conducted where oscillatory instability is encountered. At high Mach numbers and high angles of attack where minor changes in test conditions may produce large changes in the aerodynamic derivatives, a steady-state oscillation is very difficult to maintain. In situations such as this, feedback control of the oscillation should be considered as it provides a means for automatically stabilizing the amplitude and the frequency of the oscillation for any variation of damping, either positive or negative, within the capacity of the forcing system.

The system of feedback control used in the present apparatus evolved from unsuccessful experiments with the forced-oscillation technique described above at high subsonic Mach numbers. After the development of the feedback system it was found that Bratt, Raymer, and Miles in England had used a similar technique in 1942 but the results of their experiments are not generally available. The principle of operation is similar to that of the amplitude-stabilized feedback oscillator.

The oscillatory system was formed by the moment of inertia of the model and the stiffness of the restoring springs. Torque was applied to this system in the present case through a linkage with an electromagnetic shaker. It is convenient to think of the shaker system as a transducer which converts an electrical signal input into a torque. A strain gage indicating the angular deflection of the model converted the oscillation amplitude into an electrical signal. Feedback was accomplished by using amplified voltage from the strain gage as a source of electrical signal to the shaker. Velocity feedback was used in this case and the strain-gage signal of oscillation amplitude was differentiated electronically before being introduced into the shaker.

Thus, for a system with velocity feedback

$$T_{x'} = g\dot{\sigma} \tag{23}$$

and equation (4) could be written

$$I_{x'x'}\ddot{\sigma} + \left(P_{x'} - \frac{1}{4}\rho V S b^2 C_{l'_{\dot{\sigma}}} - g \right) \dot{\sigma} + \left(K_{x'} - \frac{1}{2}\rho V^2 S b\, C_{l'_{\sigma}} \right) \sigma = 0 \tag{24}$$

If g and the aerodynamic derivatives are constants, equation (24) is linear. The case of interest is where

$$P_{x'} - \frac{1}{4}\rho V S b^2 C_{l'_{\dot{\sigma}}} - g = 0 \tag{25}$$

In this case,

$$\sigma = \bar{\sigma} e^{j\omega t} \tag{26}$$

The oscillations are sinusoidal and of constant amplitude. The oscillation frequency is the undamped natural frequency, given by

$$\omega = \sqrt{\frac{K_{x'} - \frac{1}{2}\rho V^2 S b \, C_{l'_\sigma}}{I_{x'x'}}} \tag{27}$$

The peak amplitude of the oscillation, $\bar{\sigma}$, cannot be defined independently of initial conditions if the terms in equation (24) are constant as assumed. Amplitude stabilization would require that the final oscillation amplitude be independent of the initial conditions in the same sense that a "limit cycle" is independent of the starting conditions in a nonlinear oscillatory system. The transfer function, g, of the feedback loop can be designed to vary with oscillation amplitude in such a way as to produce positive feedback at low amplitudes and negative feedback at high amplitudes with a limit cycle at some intermediate amplitude. This type of stabilization, however, would appear to conflict with the requirement that g and the other coefficients in equation (24) be constants for sinusoidal motion. These conflicting requirements can be satisfied within practical limits by allowing g to vary with oscillation amplitude, but at such a slow rate that it remains essentially constant through one cycle of operation.

A rudimentary circuit of a quasi-linear element which could be inserted in the feedback loop to stabilize the amplitude of oscillation is shown schematically in figure 3(a) along with a sketch of its transfer function, figure 3(b). The thermister is the nonlinear control element. It is characterized by a high negative temperature coefficient of resistance and as current, either alternating or direct, is passed through it the resultant heating causes its resistance to change. The thermal and heat-transfer characteristics of the thermister determine the time required to reach a new resistance following a change in current. There are many variations of the principle illustrated in figure 3 which would produce an equivalent result and which can be found in the literature on amplitude stabilization of electronic oscillators.

A schematic diagram of the complete feedback control loop is shown in figure 4(a). With this system the input torque, given by $g\dot{\sigma}$, can be made equal and opposite to the damping moments acting on the model for any value of $\bar{\sigma}$ by an adjustment of the potentiometer in figure 3(a). For amplitudes less than the desired amplitude the damping moment will be less than the applied torque and oscillations will build up from rest. For amplitudes greater than desired, the damping moments will be greater than the applied torque and oscillations will decrease. The only stable operating point is where

$$P_{x'} - \frac{1}{4}\rho V S b^2 C_{l'_{\dot{\sigma}}} - g = 0 \tag{28}$$

and this can be shown to apply whether the aerodynamic damping is positive or negative.

Analog Computing System

Using the feedback control system described, the static derivatives C_{m_α}, C_{n_β}, and C_{l_β} can be determined from equation (27) and an accurate measurement of the change in oscillation frequency between the wind-on and wind-off test conditions. The equation for $C_{l'_\sigma}$ can be obtained from equation (27)

$$C_{l'_\sigma} = \frac{-2K_{x'}}{\rho V^2 S b}\left[\left(\frac{\omega}{\omega_o}\right)^2 - 1\right] \tag{29}$$

Three values of $C_{l'_\sigma}$ are required for different orientations of the axis of oscillation. Inserting these values into equation (20) with the appropriate direction cosines provides three equations for the unknowns C_{m_α}, C_{n_β}, and C_{l_β}.

Measurement of the velocity derivatives is more difficult. Early attempts to record the output of strain gages with an oscillograph and then to measure the amplitude and phase position of each trace proved to be an expensive and time-consuming task even with the aid of automatic digital computing equipment. The analog computing system discussed herein performs the same mathematical processes as the digital computing machine, but does so at the time the data are taken and results in a considerable saving in the time and expense devoted to data processing.

The measurements required in this case for a determination of the velocity derivatives were σ, $T_{x'}$, and $\epsilon_{y'}$. Each of these time-varying quantities can be represented as a Fourier series in ωt by the general expression

$$F(t) = a_o + a_1 \cos \omega t + b_1 \sin \omega t + \ldots a_n \cos n\omega t + b_n \sin n\omega t \tag{30}$$

where ω is the fundamental frequency of oscillation. Higher-order terms are always present to some degree because of buffeting of the model, wind-tunnel vibration, etc.; however, only the fundamental component in $F(t)$ is of interest. The amplitude and phase position of the fundamental can be determined from the Fourier coefficients, defined by

$$a_1 = \frac{1}{\pi}\int_{-\pi}^{\pi} F(t) \cos \omega t \, d(\omega t) \tag{31}$$

$$b_1 = \frac{1}{\pi}\int_{-\pi}^{\pi} F(t) \sin \omega t \, d(\omega t) \tag{32}$$

If strain-gage bridges are located in the oscillation apparatus in such a position as to indicate σ, $T_{x'}$, and $\epsilon_{y'}$, the output of each gage would be proportional to the product of applied voltage and gage deflection. Introducing a voltage into each gage of $\bar{e} \cos \omega t$ results in a gage output current of

$$i = k\bar{e}F(t) \cos \omega t \tag{33}$$

As in equation (30), ω is the fundamental frequency of oscillation so that upon expanding, equation (33) becomes

$$i = k\bar{e}\left(a_o \cos \omega t + \frac{a_1}{2} + \frac{a_1}{2} \cos 2\omega t + b_1 \sin \omega t \cos \omega t + \ldots\right) \tag{34}$$

A well-damped deflection galvanometer having a time constant much greater than $\frac{2\pi}{\omega}$ will not respond to currents of fundamental frequency and above. Its deflection will be proportional to the average galvanometer current, given by

$$i_{av} = \frac{1}{2\pi}\int_{o}^{2\pi} i \, d(\omega t) \tag{35}$$

With equations (34) and (35), an expression for a_1 can be obtained in terms of the average galvanometer current

$$a_1 = \frac{2i_{av}}{k\bar{e}} \tag{36}$$

Wherein i_{av} and $\bar{e}$ can be measured directly at the time of the test and k can be obtained from a static calibration of the strain gage. Similarly, b_1 can be measured using a sine wave of voltage in place of a cosine wave. The 90° phase separation between the sine and cosine voltages was obtained in this case using the input and output, respectively, of an electronic integrator. This integrator and other active components in the computing circuitry consist essentially of high gain d-c amplifiers in which the input and feedback impedances to each amplifier determine its specific function. Similar components were used in the feedback loop described previously.

A schematic diagram of the computing system used is shown in figure 4(b). The signal source for the sine and cosine voltages was the strain gage, indicating oscillation amplitude, that was used to excite the feedback loop. The reversing switch was used to apply the sine and cosine voltages alternately to each gage. These voltages were measured simultaneously with each reading by means of the rectifier circuits e_1 and e_2 and the galvanometers. The feedback loop through the attenuator was used to suppress any unusually large variations in direct current through the integrator, and the capacitors prevented this direct current from appearing at the output.

The in-phase and out-of-phase components, a_1 and b_1, respectively, of $T_{x'}$, $\epsilon_{y'}$, and σ are used to determine the maximum amplitude and relative phase position of each. Only the component of $T_{x'}$ and $\epsilon_{y'}$ in quadrature with the amplitude is required to calculate the mechanical damping and the velocity derivatives. With the notation

$$\sigma = \bar{\sigma} \sin (\omega t + \mu)$$

$$T_{x'} = \bar{T}_{x'} \sin (\omega t + \nu)$$

$$\epsilon_{y'} = \bar{\epsilon}_{y'} \sin (\omega t + \xi)$$

the velocity coefficients for each oscillation condition can be calculated from equations (4) and (7) as

$$C_{l'_{\dot{\sigma}}} = \frac{4}{\rho V S b^2} \left[P_{x'} - \frac{T_{x'} \sin (\nu - \mu)}{\omega \bar{\sigma}} \right] \tag{37}$$

$$C_{m'_{\dot{\sigma}}} = \frac{4}{\rho V S b^2} \frac{K_{y'} \epsilon_{y'}}{\omega \bar{\sigma}} \sin (\xi - \mu) \tag{38}$$

Four values of $C_{l'_{\dot{\sigma}}}$ and one of $C_{m'_{\dot{\sigma}}}$ were required in this case which, with equations (17) and (18), yielded the five rotary derivatives C_{l_p}, C_{n_p}, $C_{m_q} + C_{m_{\dot{\alpha}}}$, $C_{l_r} - C_{l_{\dot{\beta}}}$, and $C_{n_r} - C_{n_{\dot{\beta}}}$.

OPERATION

Description of Apparatus

The oscillation mechanism necessary for the dynamic tests was housed in a sting assembly which was matched to the dynamic model and the wind-tunnel model support in such a way that it was interchangeable with the stings normally used for static testing. It was thus possible to measure the static force and moment characteristics and the dynamic stability derivatives under identical test conditions.

A model airplane mounted on the oscillation equipment in the wind tunnel is shown in the photograph, figure 5. An electromagnetic shaker was housed in the enlarged portion of the sting downstream of the model airplane. Special model construction was required to obtain the necessary strength with a minimum of weight since a reduction in weight simplified many of the other design problems, particularly those relating to the supporting springs. Designed for a wing loading at high Mach numbers of approximately 400 pounds per square foot, the weight of the model in figure 5 is approximately 5 pounds per square foot of wing area.

A general view of the electronic equipment needed outside the test section is shown in the photograph, figure 6. The console on the right in the photograph is the power supply for the electromagnetic shaker housed in the model supporting sting. The panel rack on the left contains a counter for measuring frequency and the various electronic feedback and computing elements illustrated in the block diagrams, figure 4. The galvanometer and read-out system, not shown in figure 6, is the same as that normally used for static tests with a strain-gage balance.

Two oscillation mechanisms were built, one for pure pitching or yawing oscillations and one for combined rolling and pitching or rolling and yawing. A close-up view of this latter oscillation mechanism with part of the housing removed is shown in the photograph, figure 7. The crossed flexure pivots positioned the model and provided the spring restraint for the oscillatory system. Two sets of flexure pivots were built which permitted testing at two frequencies of approximately 4 and 8 cycles per second. A change in the orientation of the axis of oscillation was accomplished by rotating the apparatus about the longitudinal axis of the sting. Eight positions were available although only three are unique for the stability derivatives considered.

The strain gage indicating $\epsilon_{y'}$ was of the unbonded type since the angular deflection about the y' axis was ± 0.0005 radian or less. The deflection was held within the above limits by the radial flexures indicated as the cross-torque restraint in figure 7. This gage was required for testing in only one configuration and was mechanically disconnected for the other configurations. Because of the extremely stiff cross-torque restraint, an interaction correction was found to be necessary. It was established from a static calibration that approximately 6 percent of a moment about the x' axis was measured as a moment about the y' axis because of this interaction, and thus a correction to the measured values of $C_{m'_\sigma}$ was necessary which amounted to approximately 6 percent of the measured values of $C_{l'_\sigma}$. Other interactions were found to be negligible.

The accuracy of the data obtained is believed to be sufficient for most dynamic stability calculations. Errors directly assignable to the computing system are quite small, within 1 percent of the full-scale capacity and 1° of arc in the phase angle. Other uncertainties were caused by variations in the strain-gage calibration constants over a period of time, random aerodynamic disturbances especially at the higher angles of attack

for pitching or rolling motions, some unavoidable changes in model surface condition, mechanical damping corrections, and many other minor effects. For example, in a typical case the lateral velocity derivatives C_{l_p}, C_{n_p}, $C_{l_r} - C_{l_{\dot{\beta}}}$, and $C_{n_r} - C_{n_{\dot{\beta}}}$ were repeatable to within ±0.005 for a given set of conditions, but were subject to a total uncertainty of approximately ±0.02 as determined from repeated tests over a period of several months. Further study and experience with the test apparatus should permit the understanding and elimination of this latter type of uncertainty.

Experimental Data

Figures 8, 9, and 10 have been prepared to illustrate the general scope of data obtainable with the oscillation apparatus described. These data were obtained at a low Mach number for the model configuration illustrated in figure 5. Similar data have been obtained at Mach numbers up to 0.95.

The effects of oscillation amplitude and reduced frequency at a selected angle of attack can be studied from measurements of the type shown in figure 8. It is sometimes desirable to measure only the effect of frequency or amplitude on certain combinations of derivatives, such as $C_{n_p} + C_{l_r} - C_{l_{\dot{\beta}}}$ in figure 8, since this can be done with fewer measurements. These data confirm the assumption of linearity in the small oscillations of an airplane about an equilibrium position and indicate that the effects of frequency on the stability derivatives are negligible for the test conditions represented in figure 8.

Data of the type illustrated in figures 9 and 10 can be used to establish the variation of the stability derivatives with angle of attack for a mean oscillation amplitude and frequency as this is the form most useful in dynamic stability calculations. The data shown in figure 9, along with the lift-curve slope, are the aerodynamic parameters of primary importance in estimating the short-period dynamic longitudinal stability of an aircraft with the control surfaces fixed. The short-period motion in this case is essentially a pitching about the center of gravity combined with vertical translation. The desirability of experimentally separating $C_{m_{\dot{\alpha}}}$ and C_{m_q} and evaluating other derivatives which may affect the longitudinal motion depends on the circumstances and on the precision required but, in general, the important features of the motion can be estimated without these additional aerodynamic parameters. In the stick-free case, a third degree of freedom is introduced by the elevator motion about its hinge which may markedly affect the response of the airplane and for which the aerodynamic contribution of the free control surface would have to be considered (ref. 5).

Data of the type illustrated in figure 10 can be used in calculating the dynamic lateral stability of an airplane. Analysis of the lateral

oscillatory motion with the controls fixed is more complicated than in the longitudinal case because of the three degrees of freedom - rolling, yawing, and sideslipping. The aerodynamic parameters required, in addition to those shown in figures 10(a) and (b), are the side-force coefficients due to rolling velocity, yawing velocity, and sideslip (ref. 6). The side force due to sideslip can be measured or estimated from steady-flight considerations alone. Measured values of the side forces due to rolling velocity and yawing velocity would be desirable, but in many cases these forces are small or can be shown to have negligible effect on the motion (ref. 7). Here again, as in the case of the short-period longitudinal motion, free-control surfaces may radically alter the aircraft response (ref. 5).

Many of the suggested methods for calculating dynamic lateral stability (e.g., refs. 5, 6, and 7) do not consider the effects of sideslip velocity $\dot{\beta}$ because, for typical airplane configurations used in the past, these effects have been shown to be small (ref. 3). This may, however, not be the case for current and future airplane types. The effects of $C_{l_{\dot{\beta}}}$ and $C_{n_{\dot{\beta}}}$ on the lateral oscillatory motion can be approximated by introducing the terms $C_{l_r} - C_{l_{\dot{\beta}}}$ and $C_{n_r} - C_{n_{\dot{\beta}}}$ into the equations of motion (ref. 6) in place of C_{l_r} and C_{n_r}. This would indicate that, in the absence of independent measurements of $C_{l_{\dot{\beta}}}$ and $C_{n_{\dot{\beta}}}$, it would be desirable to obtain values of $C_{l_r} - C_{l_{\dot{\beta}}}$ and $C_{n_r} - C_{n_{\dot{\beta}}}$ from oscillation tests since this would approximately account for the possible effects of sideslip velocity in stability calculations.

Ames Aeronautical Laboratory
National Advisory Committee for Aeronautics
Moffett Field, Calif., Sept. 20, 1954

APPENDIX

General methods are available for evaluating the direction cosines for an arbitrary rotation of one system of axes with respect to another. (See, e.g., ref. 8.) In the present case it would be most useful if the direction cosines were evaluated in terms of the angles η and λ illustrated in figure 2. The angle η represents the mechanical angle by which the axis of the crossed flexures is offset from the longitudinal axis of the sting and λ is determined by keying the oscillation apparatus to the sting in the proper rotational position. The direction cosines used in equations (17), (18), and (20) then become

$$\left.\begin{aligned} A &= \cos \alpha_m \cos \eta - \sin \alpha_m \sin \eta \cos \lambda \\ B &= \sin \eta \sin \lambda \\ C &= -(\sin \alpha_m \cos \eta + \cos \alpha_m \sin \eta \cos \lambda) \\ D &= \sin \alpha_m \sin \lambda \\ E &= \cos \lambda \\ F &= \sin \lambda \cos \alpha_m \end{aligned}\right\} \tag{39}$$

In the case of the velocity derivatives, a considerable simplification in the direction cosines can be obtained by referring them to a set of model axes which coincide with the stability axes at zero angle of attack. The velocity derivatives are then evaluated first about model axes for all angles of attack and then transformed to stability axes. Inserting $\alpha_m = 0$ in the above expression for the direction cosines results in the following values for the tests reported herein, where the double primes refer to model axes

η	λ	A"	B"	C"	D"	E"	F"	Type of motion
45°	0	$1/\sqrt{2}$	0	$-1/\sqrt{2}$	not used			Rolling and yawing
45°	90°	$1/\sqrt{2}$	$1/\sqrt{2}$	0	0	0	1	Rolling and pitching
45°	180°	$1/\sqrt{2}$	0	$1/\sqrt{2}$	not used			Rolling and yawing
90°	0	0	0	-1	not used			Yawing

Use of these values for the direction cosines resulted in the determination of the velocity derivatives about model axes, using equations (17) and (18). The transformation from model axes to stability axes was made with the following equations where the double-primed coefficients refer to model axes.

$$
\left.
\begin{aligned}
C_{l_p} &= C_{l''_p} \cos^2\alpha_m + (C_{n''_r} - C_{n''_{\dot\beta}}) \sin^2\alpha_m + \\
&\qquad (C_{n''_p} + C_{l''_r} - C_{l''_{\dot\beta}}) \sin\alpha_m \cos\alpha_m \\
C_{l_r} - C_{l_{\dot\beta}} &= (C_{l''_r} - C_{l''_{\dot\beta}}) \cos^2\alpha_m - C_{n''_p} \sin^2\alpha_m + \\
&\qquad (C_{n''_r} - C_{n''_{\dot\beta}} - C_{l''_p}) \sin\alpha_m \cos\alpha_m \\
C_{n_p} &= C_{n''_p} \cos^2\alpha_m - (C_{l''_r} - C_{l''_{\dot\beta}}) \sin^2\alpha_m + \\
&\qquad (C_{n''_r} - C_{n''_{\dot\beta}} - C_{l''_p}) \sin\alpha_m \cos\alpha_m \\
C_{n_r} - C_{n_{\dot\beta}} &= (C_{n''_r} - C_{n''_{\dot\beta}}) \cos^2\alpha_m + C_{l''_p} \sin^2\alpha_m - \\
&\qquad (C_{n''_p} - C_{l''_r} + C_{l''_{\dot\beta}}) \sin\alpha_m \cos\alpha_m \\
C_{m_q} + C_{m_{\dot\alpha}} &= C_{m''_q} + C_{m''_{\dot\alpha}}
\end{aligned}
\right\} \qquad (40)
$$

The displacement derivatives C_{m_α}, C_{n_β}, and C_{l_β} were not evaluated by the above procedure as there was no computational advantage in this case. Equations (17) through (22) are developed about stability axes for which $\beta = -\psi$ and $\alpha = \theta$. The use of these same relations for the model axes system depends on the presence in equations (17) through (19) of the terms due to rolling velocity, and the advantage in using the model axes system is that thereby certain terms are eliminated in the equations and simple solutions obtained for all angles of attack. On the other hand, the use of this relation for the displacement derivatives would require the introduction of corresponding terms due to roll deflection about model axes. It can be shown that when these terms are introduced, the resulting equations are as difficult from the computing standpoint as the direct evaluation of the displacement derivatives about stability axes; therefore, in evaluating the displacement derivatives C_{m_α}, C_{n_β}, and C_{l_β}, equation (20) and the direction cosines for the stability system of axes, equation (39), were used.

It is important to note the difference between the model axes system used for equation (40) and the system of body axes used in many stability calculations. The orientation of the two systems of axes coincides but with the body axes system the sideslip angle β is defined as the angle between the relative wind and the plane of symmetry in the same manner as with the stability axes. With the approximations $\sin\sigma = \sigma$, $\cos\sigma = 1$, the sideslip angle referred to body axes would become

$$\beta = - \psi'' \cos \alpha_m + \varphi'' \sin \alpha_m$$

$$= (- C'' \cos \alpha_m + A'' \sin \alpha_m) \sigma$$

This value for β could be inserted in equations (11), (13), and subsequent equations which would lead to modifications of equations (17) through (22) and these new equations would then represent the stability derivatives referred to body axes. Therefore, while there are many similarities in the two systems, the model axes system used in equation (40) is not a true system of body axes and should be considered only as a computational aid.

REFERENCES

1. Lessing, H. C., Fryer, T. B., and Mead, M. H.: A System for Measuring the Dynamic Lateral Stability Derivatives in High-Speed Wind Tunnels. NACA TN 3348, 1954.

2. MacLachlan, Robert, and Letko, William: Correlation of Two Experimental Methods of Determining the Rolling Characteristics of Unswept Wings. NACA TN 1309, 1947.

3. Bird, John D., Jaquet, Byron M., and Cowan, John W.: Effect of Fuselage and Tail Surfaces on Low-Speed Yawing Characteristics of a Swept-Wing Model as Determined in Curved-Flow Test Section of Langley Stability Tunnel. NACA TN 2483, 1951.

4. Jones, B. Melvill: Dynamics of the Airplane. Symmetric or Pitching Moments. Vol. V of Aerodynamic Theory, div. N, ch. II, sec. 40, W. F. Durand, ed., Julius Springer (Berlin), 1935, pp. 49-50.

5. Phillips, William H.: Appreciation and Prediction of Flying Qualities. NACA Rep. 927, 1949. (Supersedes NACA TN 1670.)

6. Campbell, John P., and McKinney, Marion O.: Summary of Methods for Calculating Dynamic Lateral Stability and Response and for Estimating Lateral Stability Derivatives. NACA Rep. 1098, 1952. (Supersedes NACA TN 2409.)

7. Sternfield, Leonard, and Gates, Ordway B., Jr.: A Simplified Method for the Determination and Analysis of the Neutral-Lateral-Oscillatory-Stability Boundary. NACA Rep. 943, 1949. (Supersedes NACA TN 1727.)

8. Whittaker, Edmund Taylor: A Treatise on the Analytical Dynamics of Particles and Rigid Bodies, with an Introduction to the Problem of Three Bodies. Fourth ed., Dover Publications (New York), 1944, p. 8.

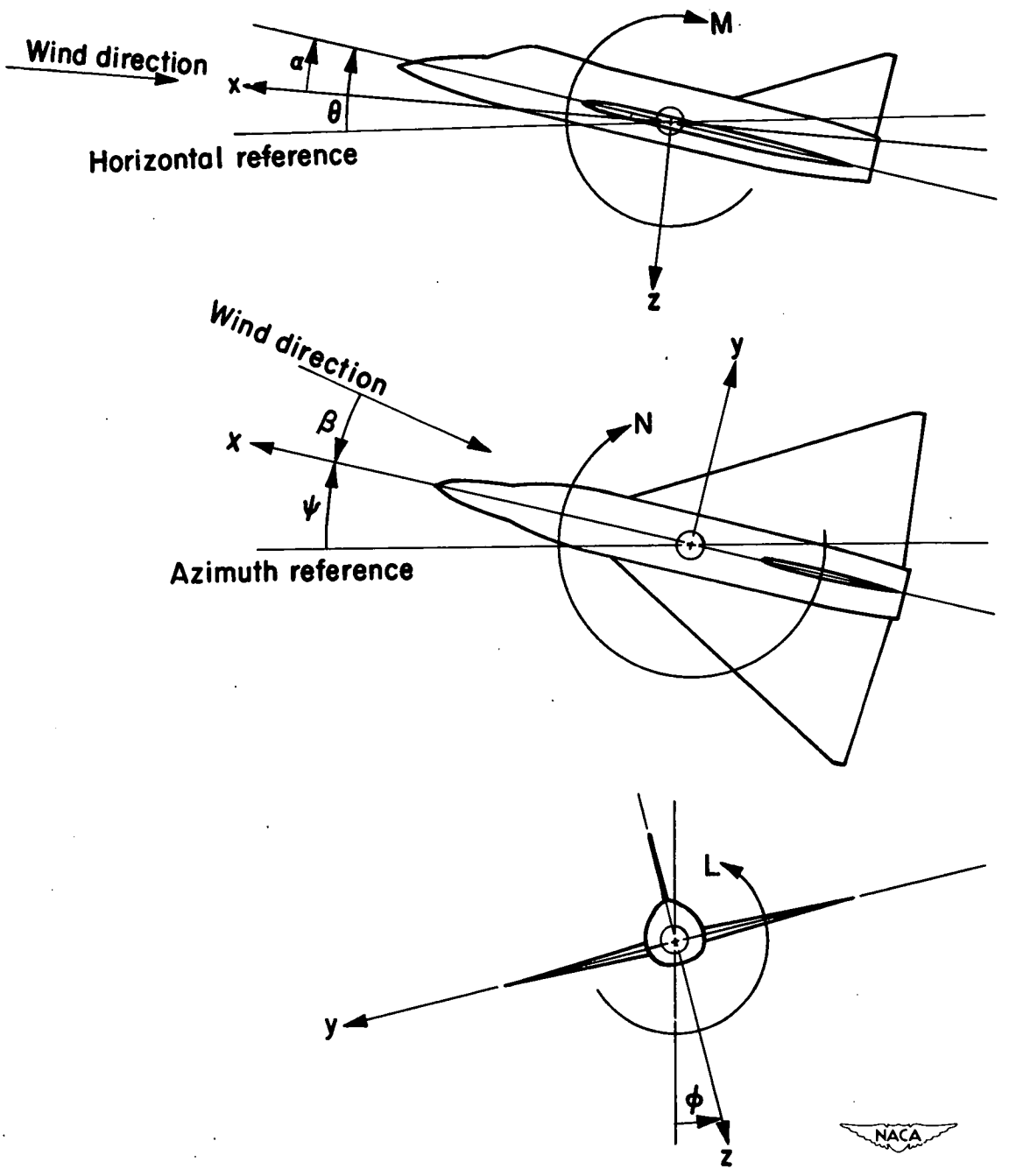

Figure 1.- The stability system of axes is an orthogonal system of axes having its origin at the center of gravity and in which the z axis is in the plane of symmetry and perpendicular to the relative wind, the x axis is in the plane of symmetry and perpendicular to the z axis, and the y axis is perpendicular to the plane of symmetry. Arrows indicate the positive directions of motions and moments.

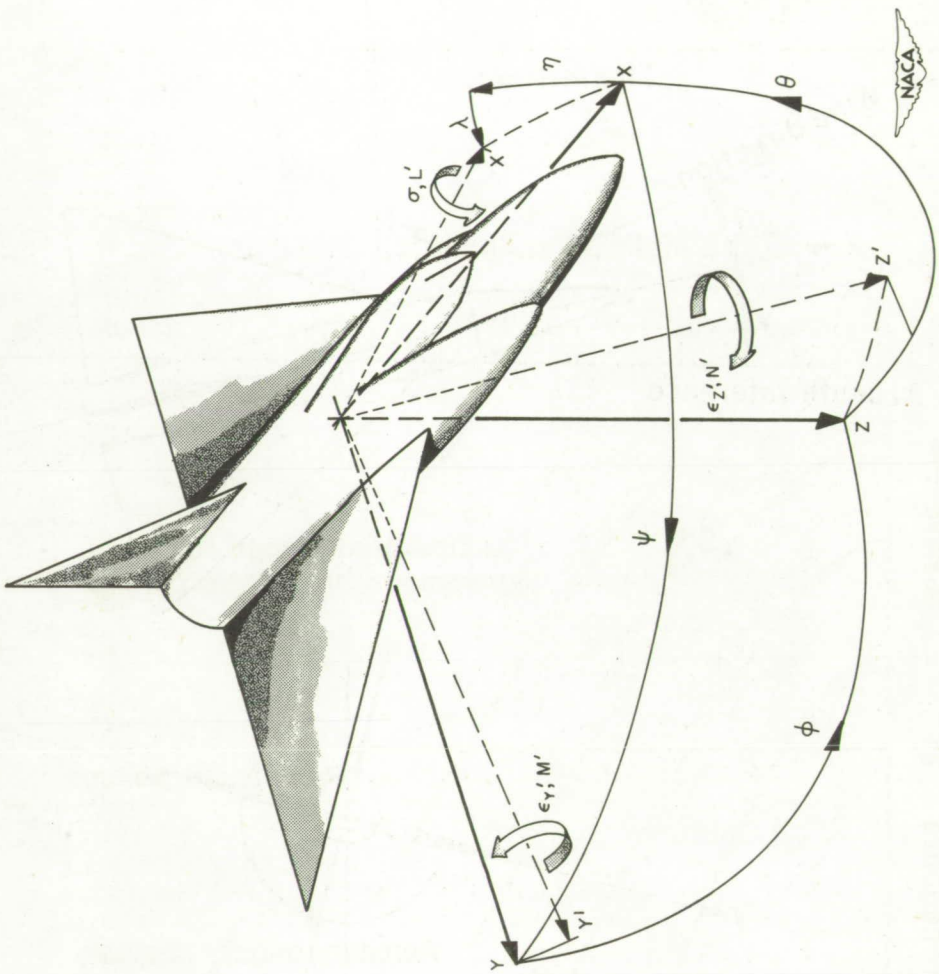

Figure 2.- The orientation of the x',y',z' system of axes is obtained by assuming an orthogonal system which is originally coincident with the stability system at zero angle of attack and with the same positive directions for forces, moments, and motions as being successively rotated about the y axis by an angle η and the x axis by an angle λ.

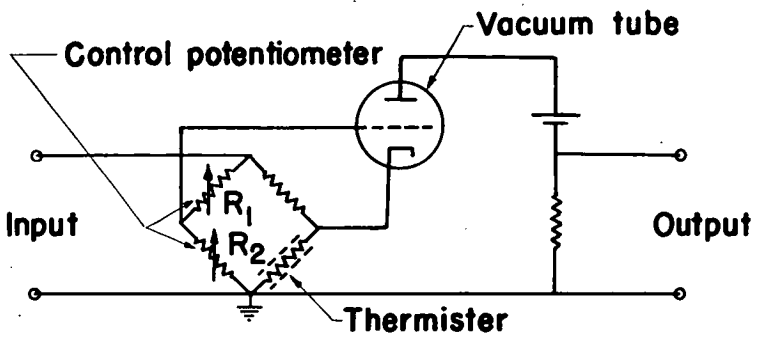

(a) Simplified schematic.

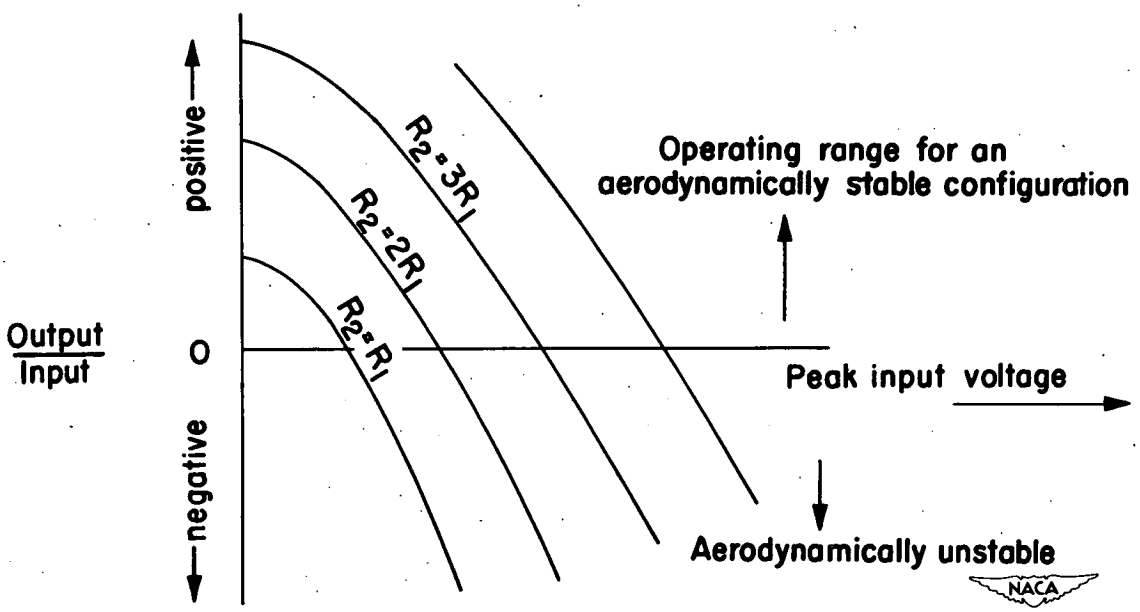

(b) Transfer function for several fixed positions of the control potentiometer.

Figure 3.- Simplified characteristics of the amplitude-control circuit.

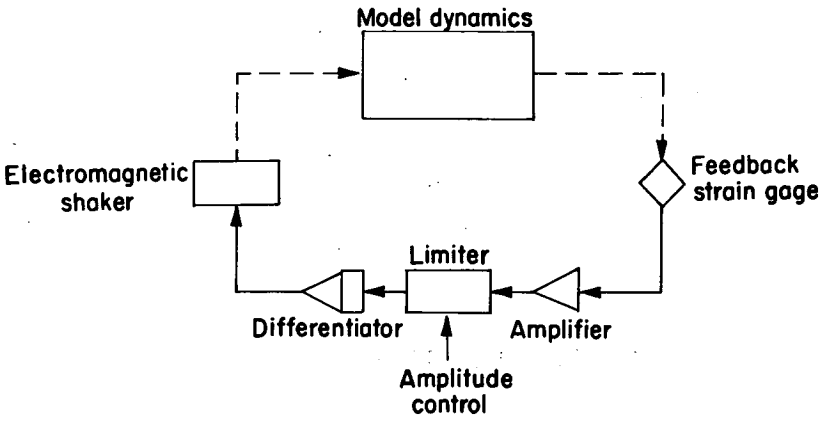

(a) Excitation system.

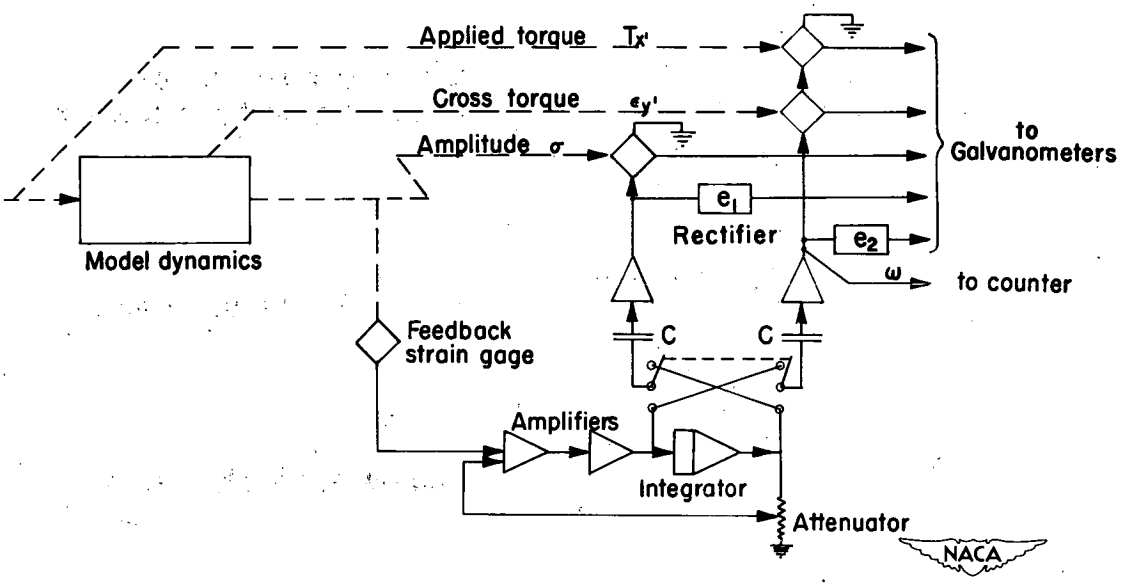

(b) Computing system.

Figure 4.- Block diagram of the excitation and computing systems.

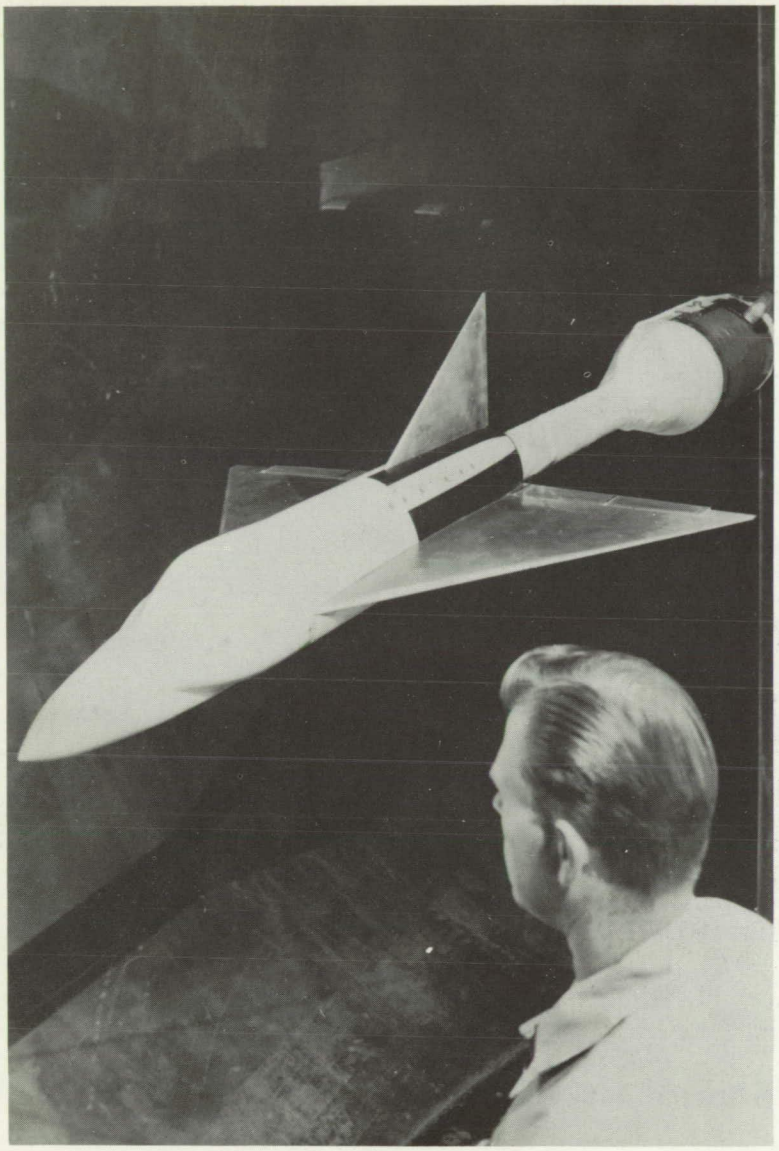

A-18500.1

Figure 5.- Model airplane installed on oscillation mechanism in wind-tunnel test section.

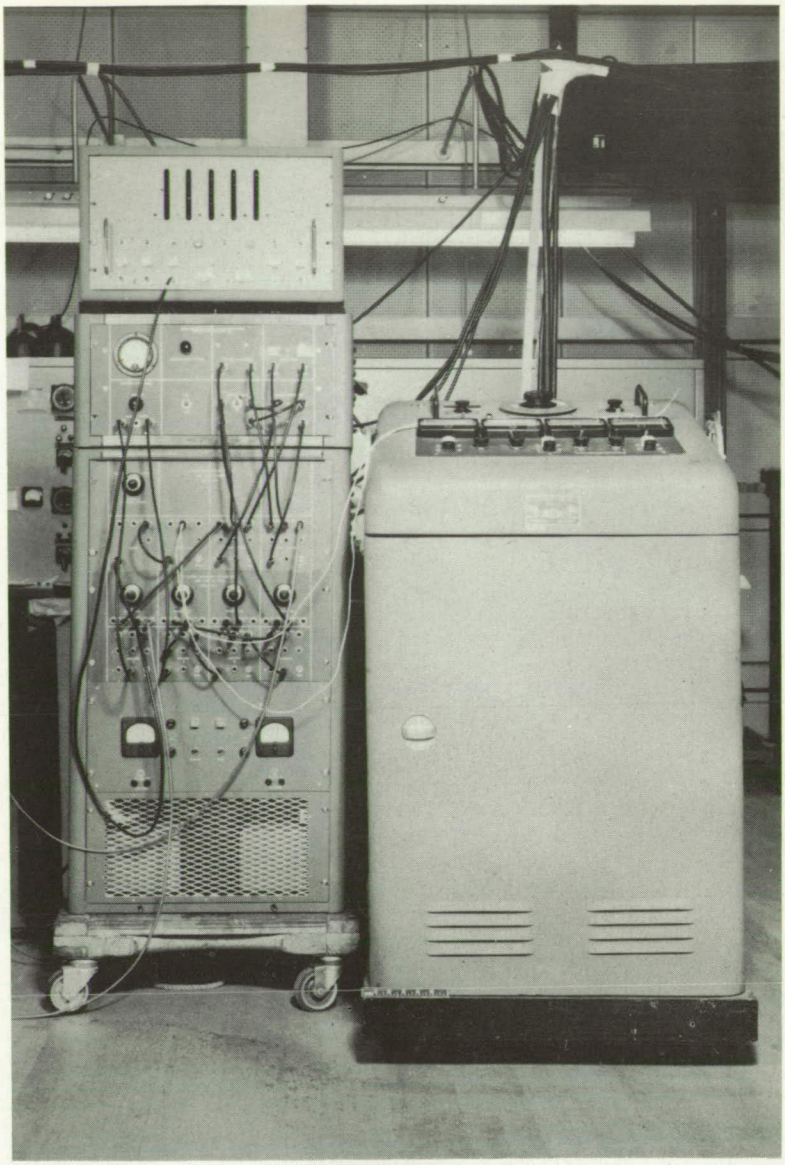

A-19366

Figure 6.- General view of electronic feedback and computing equipment used for the oscillation tests.

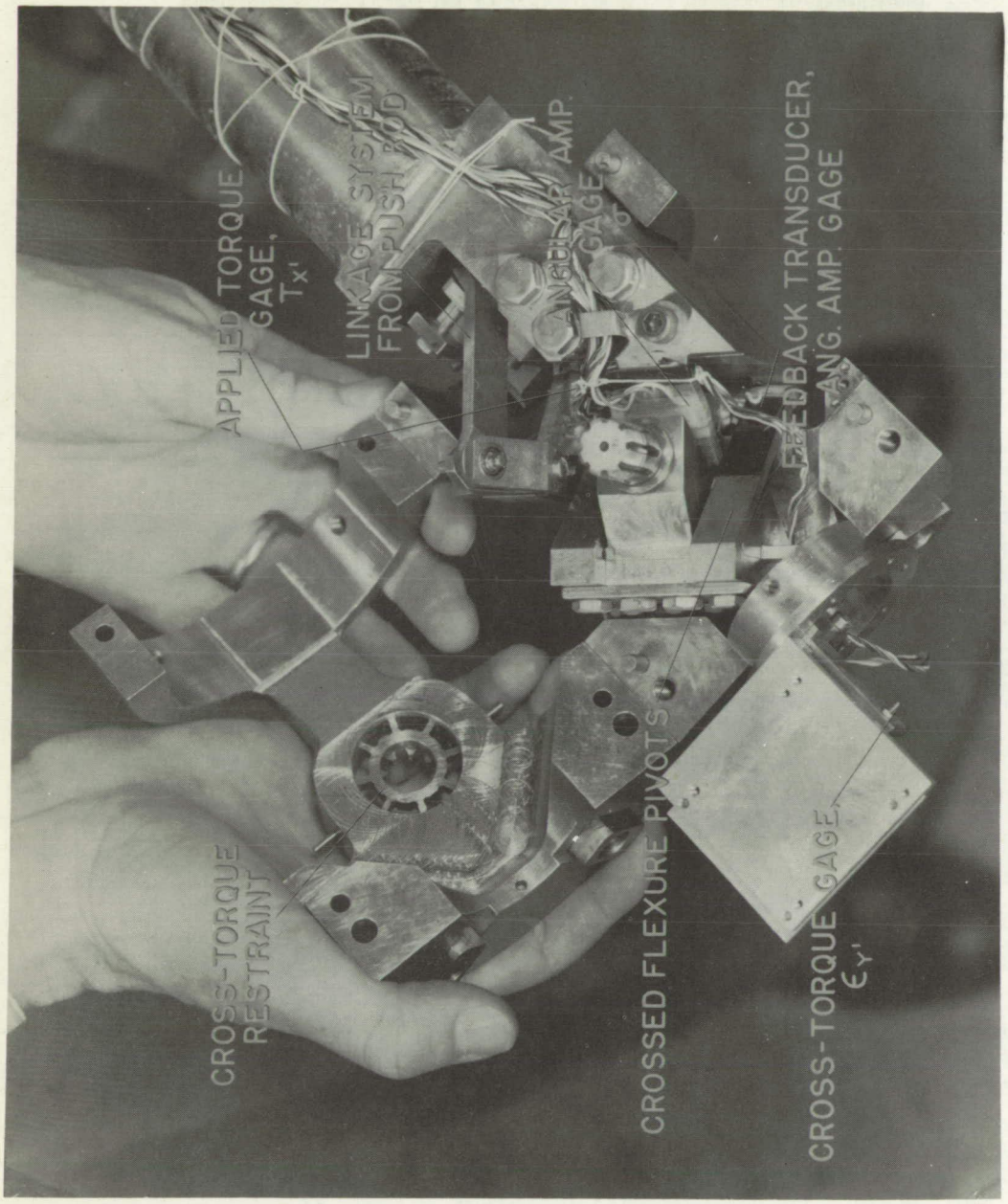

A-18665.1

Figure 7.- Oscillation mechanism with part of the housing removed.

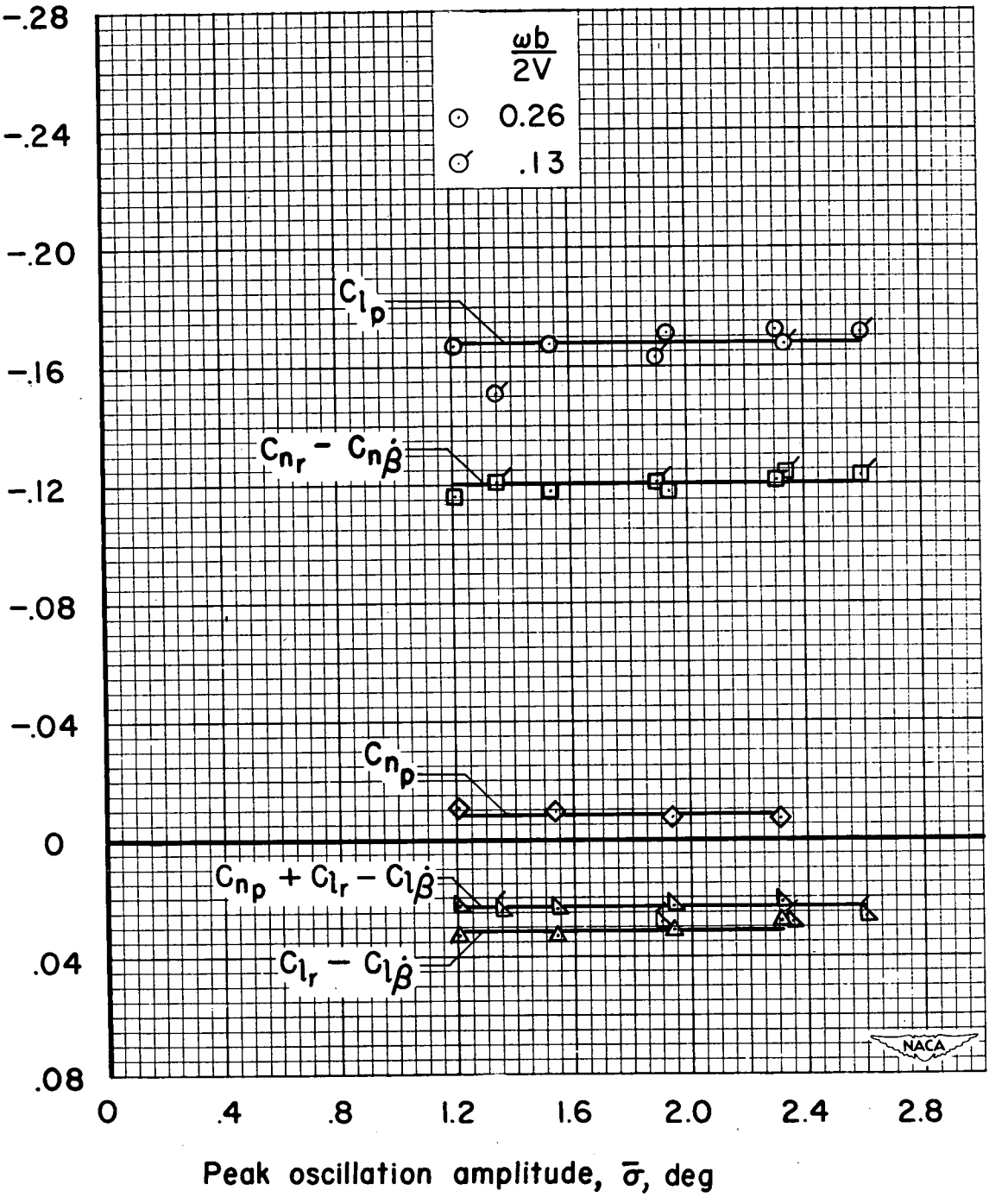

Figure 8.- The variation of some of the lateral stability derivatives with oscillation amplitude for two values of reduced frequency.

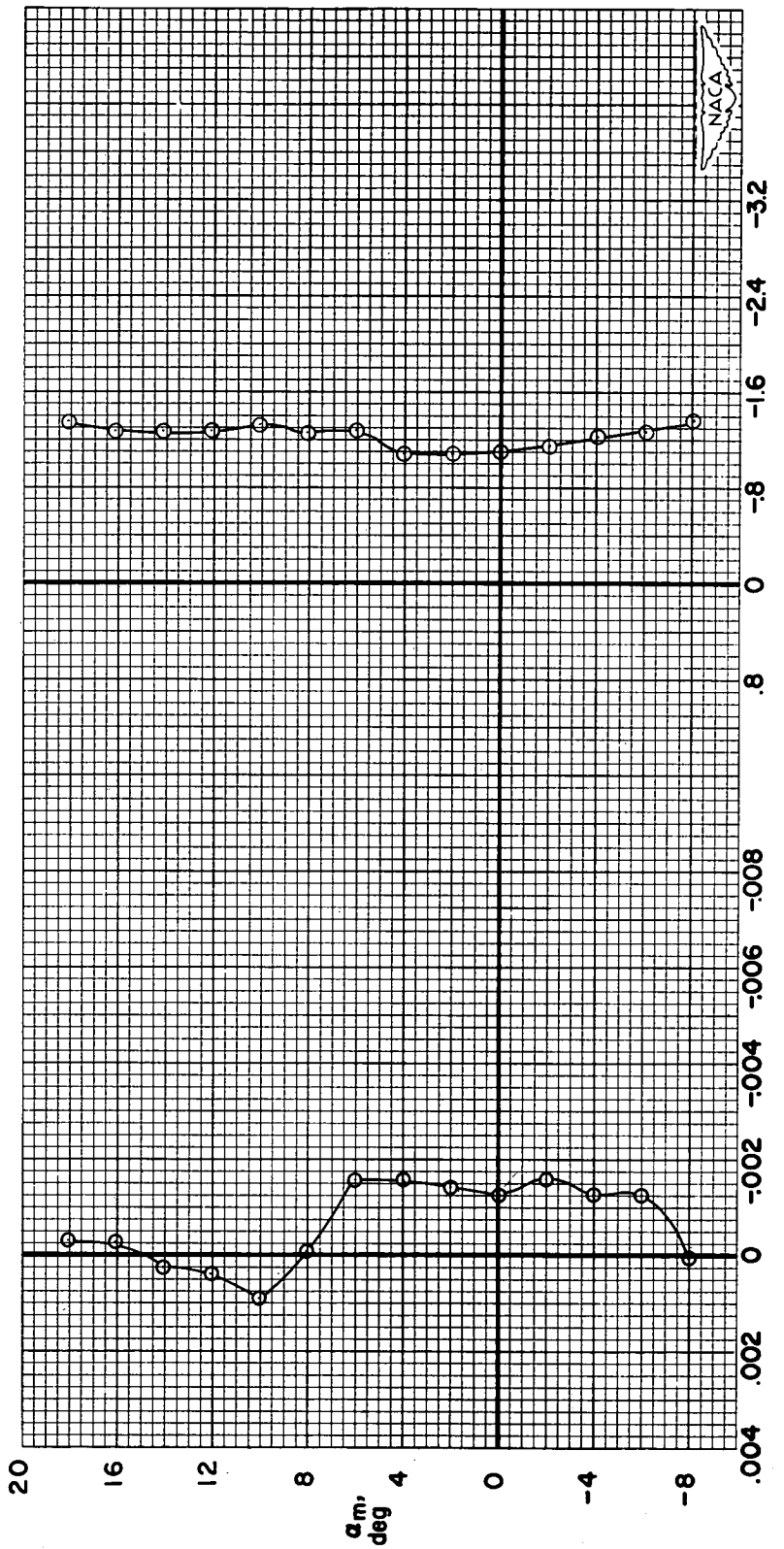

Figure 9.- The variation of the longitudinal stability derivatives with angle of attack.

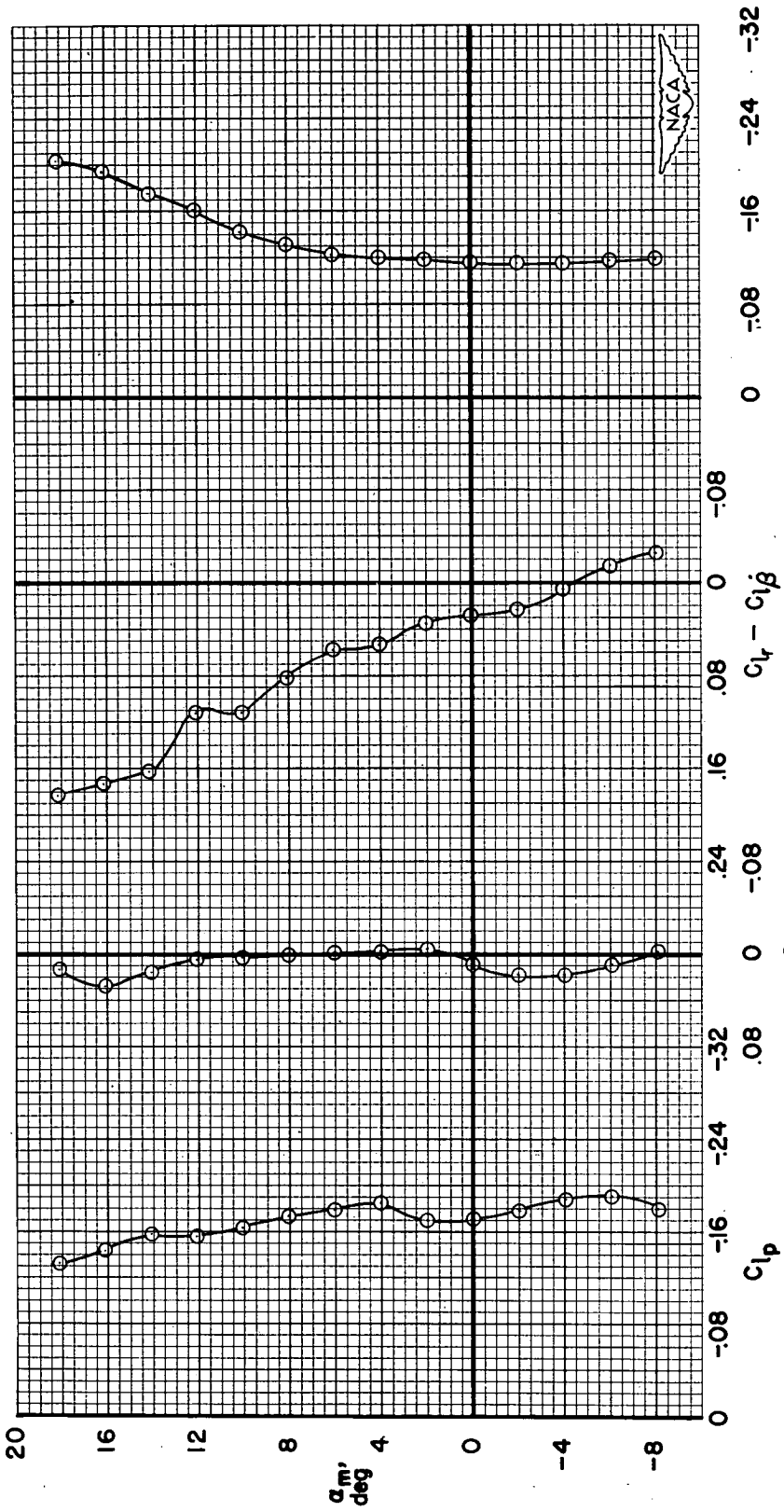

(a) C_{l_p}, C_{n_p}, $C_{l_r} - C_{l_{\dot{\beta}}}$, $C_{n_r} - C_{n_{\dot{\beta}}}$ vs. α_m

Figure 10.- The variation of the lateral stability derivatives with angle of attack.

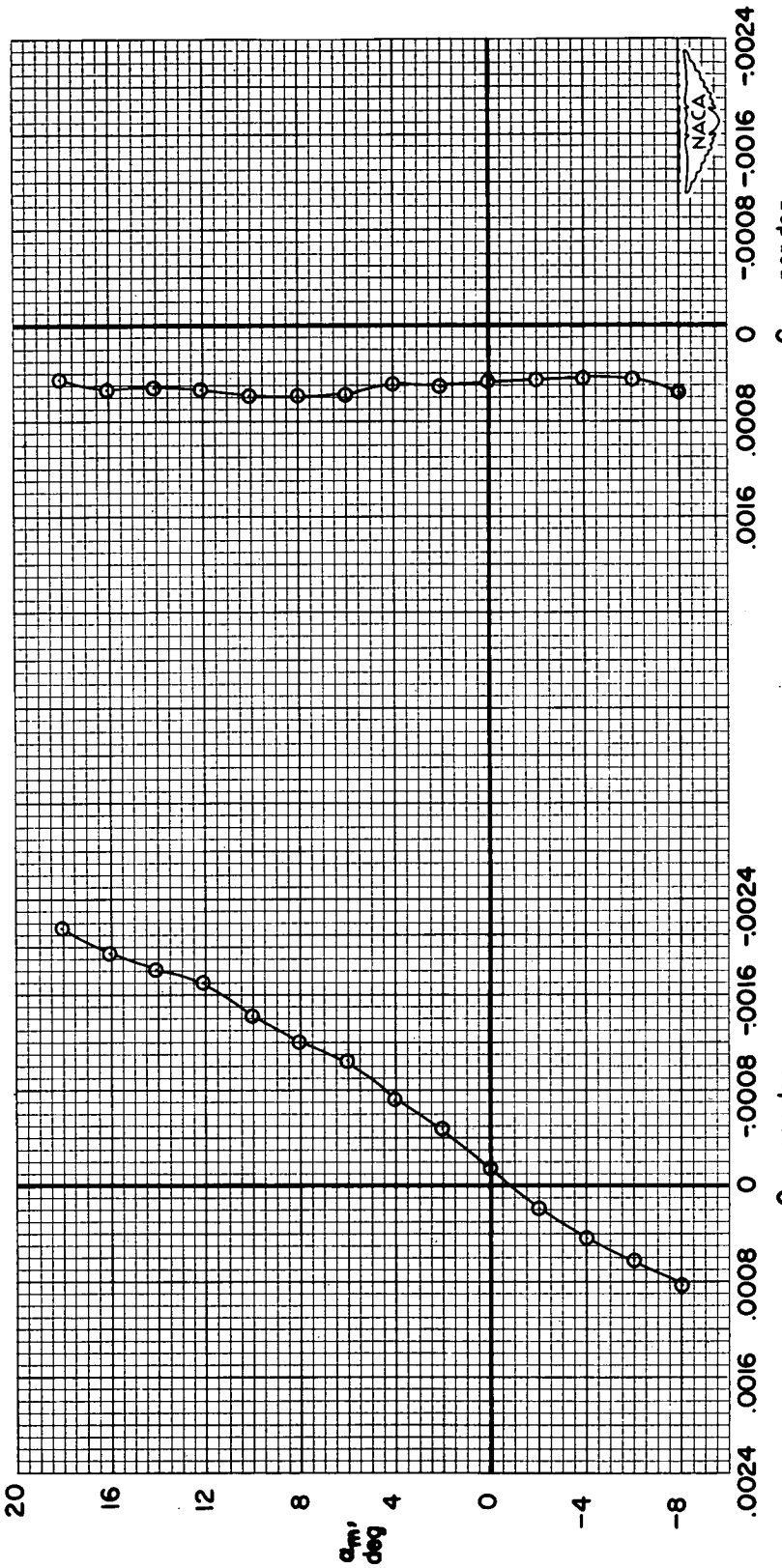

(b) C_{l_β}, C_{n_β} vs. α_m

Figure 10.- Concluded.